

Acousto-optic method of spatial frequency filtration based on diffraction of two eigenmodes of a crystal

V.M. Kotov, S.V. Averin, P.I. Kuznetsov, E.V. Kotov

Abstract. A method is proposed for two-dimensional spatial frequency filtration based on acousto-optic (AO) diffraction of two eigenmodes of a crystal on a single acoustic wave. It is shown that AO filters, based on the use of such diffraction, ensure the enhancement of the two-dimensional image edge during its optical Fourier processing. The main theoretical conclusions are experimentally confirmed using an AO paratellurite filter.

Keywords: acousto-optic diffraction, Bragg regime, optical eigenmodes of a crystal, optical image edge enhancement.

1. Introduction

Optical image edge enhancement is one of the important tasks of optical information processing (see, for example, [1]). Such an operation, first of all, significantly reduces the arrays of processed information, while preserving such important characteristics of object recognition as its shape and size.

Acousto-optic (AO) elements are widely used to solve this problem. For the first time an AO cell, as a filter of spatial frequencies, was investigated in [2]. Banerjee et al. [3] and Kotov et al. [4] demonstrated the use of this cell for one-dimensional image edge enhancement in the zeroth Bragg order, Cao et al. [5] studied image edge enhancement by means of two-stage diffraction, and Balakshy et al. [6] showed the possibility of edge enhancement of a two-dimensional image on the basis of the AO interaction tangential geometry. Balakshy and Mantsevich [7] investigated collinear diffraction for application in information processing problems, obtained transfer functions and described two-dimensional processing of optical images. Balakshy and Kostyuk [8] analysed all variants of single Bragg diffraction that can be used for edge enhancement and described a new method for visualising phase objects based on image edge enhancement. Yushkov et al. [9] considered a method of contrast enhancement using AO adaptive spatial filtering. Kostyuk [10] performed a comprehensive study of single AO interaction to process an optical image obtained in coherent light. He obtained transfer functions and analysed their character for small and large diffraction effects.

V.M. Kotov, S.V. Averin, P.I. Kuznetsov, E.V. Kotov Fryazino Branch, V.A. Kotel'nikov Institute of Radio Engineering and Electronics, Russian Academy of Sciences, pl. Akad. Vvedenskogo 1, 141190 Fryazino, Moscow region, Russia; e-mail: vmk277@ire216.msk.su

Received 15 March 2017; revision received 23 April 2017
Kvantovaya Elektronika 47 (7) 665–668 (2017)
Translated by I.A. Ulitkin

A new approach to the formation of transfer functions was proposed in [11–17], i.e. a superposition of several AO fields from different diffraction orders shifted relative to each other in the angular space. A complex of studies on AO filtration of images using second- and third-order Bragg diffraction was performed, when the transfer function of each order is a superposition of the fields of neighbouring diffraction orders. It was shown that the transfer functions are asymmetric and in the general case have a rather complex character. A technique for enhancing those parts of the field that can be used for two-dimensional image processing was developed.

In this paper we consider another regime of AO diffraction for solving such a problem. This is the AO diffraction of two eigenmodes of a crystal on an acoustic wave, the mode amplitudes being interconnected by the AO interaction. We explain the theory of this diffraction, calculate the transfer functions and present the results of fast Fourier transform processing (FFT processing) of images and the results of the experiments.

2. Theory

Figure 1 shows the vector diagrams of the proposed type of diffraction. Incident radiation with a wave vector \mathbf{K} is directed to the crystal face X at an angle α . Inside the crystal, radiation splits into two eigenmodes, \mathbf{K}_o and \mathbf{K}_e . It is assumed that the crystal is uniaxial, the optical axis direction Z being orthogonal to the optical face X . Figure 1a shows the diffraction of the eigenmode \mathbf{K}_e , and Fig. 1b – the modes \mathbf{K}_o , diffracted on the same acoustic wave with the wave vector \mathbf{q} . In Fig. 1a, the diffraction of the beam \mathbf{K}_e into the beam \mathbf{K}' is anisotropic, and the beams belong to different wave surfaces; the diffraction $\mathbf{K}_e \rightarrow \mathbf{K}''$ is isotropic, and both beams belong to the same wave surface. Similarly, in Fig. 1b, the diffraction $\mathbf{K}_o \rightarrow \mathbf{K}'$ is isotropic, and $\mathbf{K}_o \rightarrow \mathbf{K}''$ is anisotropic. In all cases, the diffraction takes place with Bragg synchronism detuning. The diffraction conditions are chosen in such a way that the diffracted beams \mathbf{K}' and \mathbf{K}'' are the same. In our case, the acoustic wave \mathbf{q} is parallel to the face X . It is assumed that the acoustic wave does not drift, and therefore the above requirement is fulfilled. The detuning vectors for the first case are $\Delta\mathbf{k}_1$ and $\Delta\mathbf{k}_2$, for the second – $\Delta\mathbf{k}_3$ and $(\Delta\mathbf{k}_1 + \Delta\mathbf{k}_2 + \Delta\mathbf{k}_3)$. We have separately presented the interaction events, so as not to overload the overall picture.

As can be seen from Fig. 1, both isotropic and anisotropic types of diffraction are possible; therefore, it is assumed that both diffraction geometries exist. In particular, when a single TeO_2 single crystal is used as an AO medium, this is done if light propagates near the optical axis of the crystal, which, for example, makes it possible to realise a third-order interaction

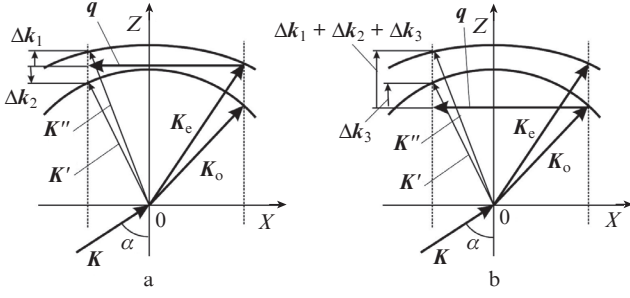


Figure 1. Vector diagrams of AO diffraction of the crystal eigenmodes.

in TeO₂. As was shown in [18, 19], the corresponding effective photoelastic constants in TeO₂ differ only by a factor of two. This will be used by us in the calculations.

The beams K_o and K_e form the zeroth Bragg order, the beams K' and K'' – the first order. The amplitudes of the fields of diffraction orders are found from the system of differential equations, which is easy to obtain according to the technique developed in [18]. In our case, the system of equations has the form:

$$\begin{aligned} \frac{dc_{01}}{dz} &= -\frac{w_i}{2}c_{11}\exp(-i\Delta k_1 z) - \frac{w_a}{2}c_{12}\exp(-i\Delta k_2 z), \\ \frac{dc_{02}}{dz} &= -\frac{w_i}{2}c_{12}\exp(-i\Delta k_3 z) \\ &\quad - \frac{w_a}{2}c_{11}\exp[-i(\Delta k_1 + \Delta k_2 + \Delta k_3)z], \\ \frac{dc_{11}}{dz} &= \frac{w_i}{2}c_{01}\exp(i\Delta k_1 z) \\ &\quad + \frac{w_a}{2}c_{02}\exp[i(\Delta k_1 + \Delta k_2 + \Delta k_3)z], \\ \frac{dc_{12}}{dz} &= \frac{w_i}{2}c_{02}\exp(i\Delta k_3 z) + \frac{w_a}{2}c_{01}\exp(i\Delta k_2 z), \end{aligned} \quad (1)$$

where c_{01} , c_{02} , c_{11} and c_{12} are the amplitudes of the fields corresponding to the beams K_e , K_o , K'' and K' ; z is the direction along which the AO interaction develops; and w_i and w_a are the parameters describing the dependence of the isotropic and anisotropic diffraction events on the acoustic power. They are defined [18, 20] as

$$w_{i,a} = \frac{2\pi}{\lambda} \frac{1}{\cos\theta} \sqrt{\frac{M_{2(i,a)}}{2HL}} P_a. \quad (2)$$

Here, λ is the wavelength of light; θ is the angle between the direction of propagation of light in the crystal and the front of the acoustic wave; H is the height of the acoustic column; L is the length of the AO interaction; and P_a is the acoustic wave power. The AO coefficient of material quality is

$$M_{2(i,a)} = \frac{n_1^3 n_2^3 p_{\text{eff}(i,a)}^2}{\rho V^3}, \quad (3)$$

where n_1 and n_2 are the refractive indices of the incident and diffracted beams, respectively; $p_{\text{eff}(i)}$ and $p_{\text{eff}(a)}$ are the effective photoelastic constants for isotropic and anisotropic diffrac-

tion events; and ρ and V are the density of the crystal and the velocity of the acoustic wave.

It is assumed that the amplitudes for the beams K_o and K_e before entering the region of the AO interaction are equal, and so in solving system (1) we use the boundary conditions

$$c_{01} = c_{02} = 1/\sqrt{2}, \quad c_{11} = c_{12} = 0 \quad \text{for } z = 0. \quad (4)$$

The method of solving a system of first-order differential equations is standard and can be found, for example, in [21].

We will consider diffraction in a TeO₂ crystal. Since the crystal is gyrotropic, its eigenwaves are elliptically polarised. When light propagates near the optical axis of the crystal, which is implied in our case, the polarisation of the waves is close to circular. The electric fields of the eigenwaves K_e and K_o will be taken in the form [22]

$$\mathbf{E}_e = \frac{c_{01}}{\sqrt{2}} [e_1 \sin(\omega t) + e_2 \cos(\omega t)], \quad (5)$$

$$\mathbf{E}_o = \frac{c_{02}}{\sqrt{2}} [-e_1 \sin(\omega t + \varphi_0) + e_2 \cos(\omega t + \varphi_0)],$$

where e_1 and e_2 are the unit vectors along the directions orthogonal to K_e and K_o (in the calculations it was assumed that e_1 is directed orthogonally to the diffraction plane containing X and Z directions (Fig. 1), e_2 is orthogonal to e_1 and K_e , K_o); ω is the frequency of light; t is the time; and φ_0 is the phase difference of the beams arising at the exit of the crystal due to the difference in the propagation velocities of the beams K_e and K_o in an anisotropic medium. The refractive indices of the beams of a uniaxial gyrotropic crystal were defined [23] as

$$n_{1,2}^2 = 1 + \tan^2 \Theta \quad (6)$$

$$\times \left[\frac{1}{n_o^2} + \frac{\tan^2 \Theta}{2} \left(\frac{1}{n_o^2} + \frac{1}{n_e^2} \right) \pm \frac{1}{2} \sqrt{\frac{\tan^4 \Theta}{2} \left(\frac{1}{n_o^2} - \frac{1}{n_e^2} \right)^2 + 4G_{33}^2} \right]^{-1},$$

where Θ is the angle between the optical axis Z of the crystal and the direction of the wave vector of light; n_o and n_e are the main refractive indices of the crystal; and G_{33} is the component of the gyration pseudotensor. For the calculations, we used: $\lambda = 0.63 \mu\text{m}$, $n_o = 2.26$, $n_e = 2.41$, $G_{33} = 2.62 \times 10^{-5}$, $L = 0.6 \text{ cm}$, $H = 0.4 \text{ cm}$, $\theta \approx 0$. The crystal length along the Z axis was 1.0 cm.

It is known [24] that in combining two circularly polarised waves, rotating in opposite directions and having identical amplitudes, a linearly polarised wave is formed. If the velocities of the waves are different, then the angle of rotation of the total polarisation varies as a function the crystal length. In addition, if the wave amplitudes are not equal to each other [i.e., $c_{01} \neq c_{02}$ in (5)], then the total wave will be elliptically polarised rather than linear. We assumed in the calculations that a polariser was installed at the crystal output, separating a linearly polarised component of the total radiation at one or another orientation of the polariser. The orientation of the polariser was set by the angle α , measured from the propagation direction of the acoustic wave. As the analysis shows, the use of a polariser significantly improves the characteristics of the AO filter.

Figure 2 shows as an example the transfer function (field distribution of the AO interaction) of the zeroth Bragg order, calculated by solving system (1) with allowance for (2)–(6) at

$\alpha = 100^\circ$ and $P_a = 1.5$ W. It was assumed that diffraction occurs on a 'slow' acoustic wave with a frequency of 26 MHz, propagating in TeO_2 at 0.617×10^5 cm s^{-1} . The angular size of the reduced field is $15^\circ \times 15^\circ$. The field represents a family of circles with a single centre and separate nonuniform regions caused by the AO interaction. Two regions of $2^\circ \times 2^\circ$ are shown by squares, which, according to our analysis, are suitable for obtaining a two-dimensional image edge. The regions are arranged symmetrically with respect to the symmetry axis $O-O'$ of the field distribution. We should note that in this case the transfer function of the zeroth order is formed by two different physical mechanisms, i.e. the conoscopic effect and the acousto-optic interaction.

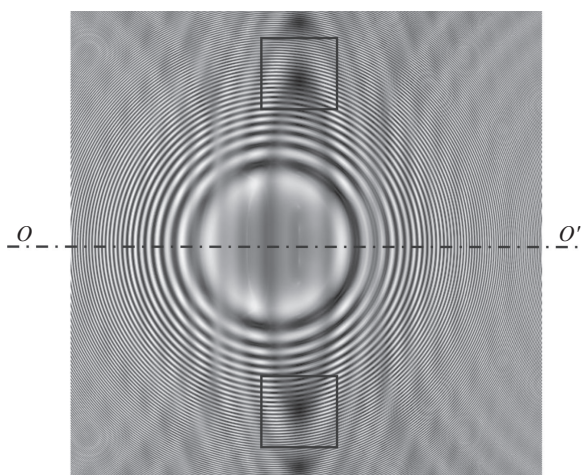


Figure 2. Transfer function of the zeroth diffraction order. Squares show the regions that allow a two-dimensional image edge to be formed.

Figure 3 shows as an example a rectangular image before and after FFT processing. The filter was one of the selected regions of Fig. 2. It can be seen that the image in Fig. 3b has a well-defined two-dimensional edge. Inside the edge the field is not quite 'suppressed', and there is some gray background. We associate this with the nonuniformity of the transfer function, which in some directions quite well suppresses spatial frequencies, and in others – does not. The average level of the residual background we estimate to be $\sim 20\%$. Thus, the error of the method is 20%.



Figure 3. (a) Original image and (b) its appearance after FFT processing using the selected region in Fig. 2 as a spatial frequency filter.

3. Experiment and discussion of its results

The optical scheme of the experimental setup is shown in Fig. 4.

As a processed image located in the input plane IP, a rectangular hole was chosen, representing a slit with a size of

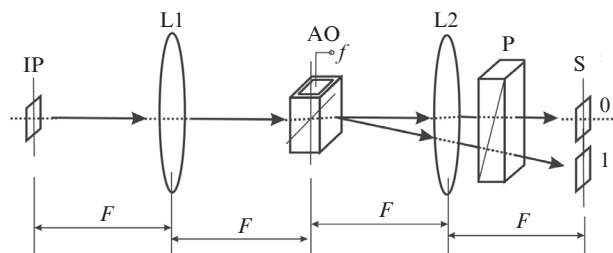


Figure 4. Optical scheme of the experimental setup: (IP) input plane; (L1, L2) lenses with a focal length F ; (AO) acousto-optic cell to which a signal with a frequency f is applied; (P) polariser; (S) screen with images in the zeroth (0) and first (1) diffraction orders.

1×1.5 mm, which was illuminated from one side by an extended He–Ne laser beam ($\lambda = 0.63$ μm). The image was directed to a system of two lenses, L1 and L2, operating according to the $4F$ scheme, where F is the focal length of the lenses (in our experiments $F = 16$ cm). The distance between the lenses was $2F$. The rectangular hole was in front of the first lens at a distance F from it. Between the lenses an AO cell was placed, performing the function of a spatial frequency filter. Behind the second lens, at a distance F from it, the screen S was located, on which the output images in the zeroth (0) and first (1) diffraction orders were observed. Between the lens L2 and the output screen there was a polariser P. In the experiments we used a standard AO cell made of a TeO_2 single crystal. Along the [110] direction of the crystal, there propagated a transverse acoustic wave excited by a piezoelectric transducer made of LiNbO_3 , to which a microwave signal with a frequency f was fed. The AO interaction length was 0.6 cm, the size of the transducer was 0.6×0.4 cm. A 'slow' wave propagated in the crystal (at a velocity of 617 m s^{-1}), and optical radiation was directed at a small angle to the optical axis [001] of the crystal. In this case, isotropic and anisotropic diffraction of light on the sound was realised in the crystal. When selecting the voltage of the high-frequency signal supplied to the converter (in our case, the optimum voltage was 7.8 V), the angular orientation of the AO cell, the sound frequency of 26.6 MHz and the angle of polariser inclination of $\alpha \approx 45^\circ$, we clearly observed a two-dimensional image edge in the zeroth order of diffraction on the screen.

Figure 5 shows photographs of a rectangular image in the zeroth and first Bragg orders, obtained as a result of diffraction. It can be seen that in the zeroth order a well-defined edge of the rectangular image is observed. The edge is formed quite qualitatively both in the vertical and horizontal directions. There is a background inside the pattern edge, indicating insufficient filtering of spatial frequencies. This can be caused both by the error of the method and by the inhomogeneity of the AO cell material, leading to distortions of the optical and acoustic fields inside the crystal. In any case, the edge is fairly clearly expressed, which confirms the possibility of using the proposed mechanism for the formation of a transfer function for two-dimensional processing of optical images.

On the basis of the results obtained, we can conclude that there is good agreement between the theoretical and experimental data. A certain discrepancy between them (a small difference in the acoustic frequencies, the angular orientation of the output polariser, etc.) can be due to a number of factors (the inaccuracy of the model describing the gyrotropic crystal, the divergence of sound or the inaccuracy of the orientation of the crystal faces, the inhomogeneity of the AO medium, etc.).

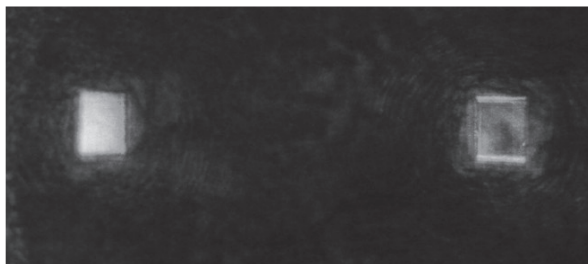


Figure 5. Photos of the image on the screen after its FFT processing. The image on the right is obtained in the zeroth diffraction order, and the image on the left – in the first diffraction order.

4. Conclusions

Based on the results obtained, we can draw the following conclusions.

1. To enhance the edges of a two-dimensional image using the AO cell as a filter of spatial frequencies it is proposed to use the regime of two-mode AO diffraction, when two modes of the incident radiation and two modes of the first-order diffracted beam are involved in the AO interaction.

2. Calculations are performed based on the theory of coupled modes. The transfer functions are obtained. The regions of transfer functions are found that provide the edge enhancement of a two-dimensional optical image. Using the results of FFT processing of optical images, it is found that the nonuniformity of the working regions of the transfer functions does not provide complete filtering of the central part of the images. The average background level inside the edges is $\sim 20\%$.

3. It is experimentally demonstrated that the image edge is enhanced in the zeroth diffraction order when FFT processing of the optical image is employed, where the filter of spatial frequencies is a cell made of a TeO_2 single crystal.

The unevenness of the image edge resulting from the optical FFT processing of the image is due to the peculiarities of the generated transfer function, namely, its nonuniformity and insufficient symmetry. Some disadvantages of the proposed mechanism include its less adaptability in the selection of high-order spatial harmonics, since the values of the detuning vectors for the two types of diffraction have a different frequency dependence. The observed background within the image edges can be due to both the insufficient accuracy of the method used and the nonuniformity of the AO cell material.

The advantages of the method include fairly simple implementation, i.e., the possibility of its application on the basis of AO cells made of TeO_2 at frequencies of 20–80 MHz in geometries that exclude the drift of an acoustic wave.

The obtained results substantially expand the possibilities of using AO cells for optical image processing tasks, in particular, for image edge enhancement.

Acknowledgements. The work was partially supported by Russian Foundation for Basic Research (Grant Nos 15-07-0231, 16-07-00064).

References

1. Young T.Y., Fu K.-S. (Eds) *Handbook of Pattern Recognition and Image Processing* (New York: Acad. Press, Inc., 1986).

2. Balakshy V.I. *Radiotekh. Elektron.*, **29**, 1610 (1984).
3. Banerjee P.P., Cao D., Poon T.-C. *Appl. Opt.*, **36**, 3086 (1997).
4. Kotov V.M., Shkerdin G.N., Shkerdin D.G., Kotov E.V. *Radiotekh. Elektron.*, **54**, 747 (2009).
5. Cao D., Banerjee P.P., Poon T.-C. *Appl. Opt.*, **37**, 3007 (1998).
6. Balakshy V.I., Voloshinov V.B., Babkina T.M., Kostyuk D.E. *J. Modern Opt.*, **52**, 1 (2005).
7. Balakshy V.I., Mantsevich S.N. *Opt. Spektrosk.*, **103**, 831 (2007).
8. Balakshy V.I., Kostyuk D.E. *Appl. Opt.*, **48**, C24 (2009).
9. Yushkov K.B., Molchanov V.Ya., Belousov P.V., Abrosimov A.Yu. *J. Biomed. Opt.*, **21**, 016003 (2016).
10. Kostyuk D.E. Cand. Diss. (Moscow, Moscow State University, 2008).
11. Kotov V.M., Averin S.V., Shkerdin G.N., Voronko A.I. *Quantum Electron.*, **40**, 368 (2010) [*Kvantovaya Elektron.*, **40**, 368 (2010)].
12. Kotov V.M., Shkerdin G.N., Bulyuk A.N. *Quantum Electron.*, **41**, 1109 (2010) [*Kvantovaya Elektron.*, **41**, 1109 (2010)].
13. Kotov V.M., Shkerdin G.N., Averin S.V., Kotov E.V. *Prikl. Fiz.*, **3**, 5 (2012).
14. Kotov V.M., Shkerdin G.N., Averin S.V. *Radiotekh. Elektron.*, **12**, 57 (2012).
15. Kotov V.M., Shkerdin G.N., Grigoryevsky V.I. *Radiotekh. Elektron.*, **58**, 226 (2013).
16. Kotov V.M., Shkerdin G.N. *Radiotekh. Elektron.*, **58**, 1040 (2013).
17. Kotov V.M., Shkerdin G.N., Averin S.V. *Radiotekh. Elektron.*, **61**, 1090 (2016).
18. Balakshy V.I., Parygin V.N., Chirkov L.E. *Fizicheskie osnovy akustooptiki* (Physical Principles of Acousto-optics) (Moscow: Radio i svyaz', 1985).
19. Voloshinov V.B., Parygin V.N., Chirkov L.E. *Vestn. Mosk. Univer., Ser. Fiz. Astron.*, **17** (3), 305 (1976).
20. Magdich L.N., Molchanov V.Ya. *Acousto-optic Devices and Their Applications* (New York: Gordon and Breach Science Publishers, 1989; Moscow: Sov. radio, 1978).
21. Piskunov N.S. *Differential and Integral Calculus* (New Delhi: CBS Publishers and Distributors, 1999; Moscow: Nauka, 1970) Vol. II.
22. Yariv A., Yeh P. *Optical Waves in Crystals* (New York: Wiley, 1984; Moscow: Mir, 1987).
23. Kotov V.M. *Akustooptika. Breggovskaya difraktsiya mnogotsvetnogo izlucheniya* (Acousto-optics. Bragg Diffraction of Multicolor Radiation) (Moscow: Yanus-K, 2016).
24. Born M., Wolf E. *Principles of Optics* (New York: Pergamon Press, 1980; Moscow: Nauka, 1973).